

---

---

COMBUSTION, EXPLOSION,  
AND SHOCK WAVES

---

---

## Combustion and Detonation of Mechanoactivated Aluminum–Potassium Perchlorate Mixtures

A. Yu. Dolgoborodov<sup>a, b</sup>, B. S. Ermolaev<sup>c</sup>, A. A. Shevchenko<sup>b</sup>, V. A. Teselkin<sup>c</sup>,  
V. G. Kirilenko<sup>c</sup>, K. A. Monogarov<sup>c</sup>, and A. N. Streletskii<sup>c</sup>

<sup>a</sup> Joint Institute for High Temperatures, Russian Academy of Sciences, Moscow, Russia

<sup>b</sup> National Research Nuclear University “MEPhI”, Moscow, Russia

<sup>c</sup> Semenov Institute of Chemical Physics, Russian Academy of Sciences, Moscow, Russia

e-mail: aldol@chph.ras.ru

Received May 20, 2014

**Abstract**—The properties of mechanoactivated energetic composites based on aluminum and potassium perchlorate with high rates of self-sustaining chemical reactions under conditions of combustion and detonation are examined. The results of experiments on studying the combustion, deflagration-to-detonation transition, and sensitivity to friction of these composites are reported. The activation duration and aluminum content in the mixture are varied. The experiments on the deflagration-to-detonation transition of mechanoactivated composites are supplemented by the results of numerical simulations. The calculations and experiments on the dynamics of development of a blast wave and on the steady detonation velocity are found to be in qualitative agreement. It is shown that the velocity of the observed process is significantly (by about 40%) lower than the normal detonation velocity obtained from thermodynamic calculations.

**Keywords:** mechanoactivation, potassium perchlorate, aluminum, deflagration-to-detonation transition

**DOI:** 10.1134/S1990793115040041

### INTRODUCTION

Currently, various research centers actively work on developing new ways to produce energetic materials with high-rate energy release. One such method involves the mechanochemical treatment of micron-sized oxidizer–fuel mixtures in ball mills. The components are crushed to submicron sizes and mixed, a process accompanied by the formation of defects in the crystal structure of the materials. Previous results on the mechanoactivation of such mixtures [1–4] have demonstrated the prospects of this direction for producing mechanoactivated energetic composites (MAEC) with high-rate self-sustaining chemical reactions during burning and detonation.

This paper reports the results of a study aimed at creating MAEC based on aluminum and potassium perchlorate (KClO<sub>4</sub>, PP). The results of experiments on studying the burning and deflagration-to-detonation transition of such mixtures and on their sensitivity to friction are presented. In the experiments, the duration of activation and the aluminum content in the mixture were varied. The experiments on the deflagration-to-detonation transition in mechanoactivated composites were supplemented by numerical simulations and thermodynamic calculations of the detonation parameters of the mixtures.

### EXPERIMENTAL RESULTS

The starting materials for preparation of the mixtures were chemically pure PP powder (50–100- $\mu\text{m}$  grains) and aluminum powders (PP-2 grade, with flaky particles, 50–200  $\mu\text{m}$  in transverse size and 2–5  $\mu\text{m}$  in thickness, and ASD-6, with spherical particles of average size  $\sim 3.6$   $\mu\text{m}$ ). The weight content of Al in the mixture was varied from 30 to 40%, near the stoichiometric weight ratio of the Al/PP components, equal to 34.2/65.8.

The mixing and activation of the components was carried out in an Activator-2SL planetary mill (ZAO “Activator”, Novosibirsk) with steel balls and drums. The weight of the mixture was 10 g, whereas that of the balls was 300 g. The most important aspect of mechanoactivation is to prevent the explosion of the mixture, so it is necessary to create a liquid layer between the components in order to reduce frictional heating and overheating of the drums. To this end, the hexane was added to the mixture, and the processing was carried out under water-cooling of the drums in 60-s cycles. The total activation time  $T_{\text{act}}$  ranges from 2 to 60 min. After treatment, the product was dried. Since the product contained relatively large agglomerates after drying, it was sieved through a 0.4-mm-mesh sieve. The starting materials and mechanoactivated composites were analyzed by X-ray diffraction and scanning electron microscopy.

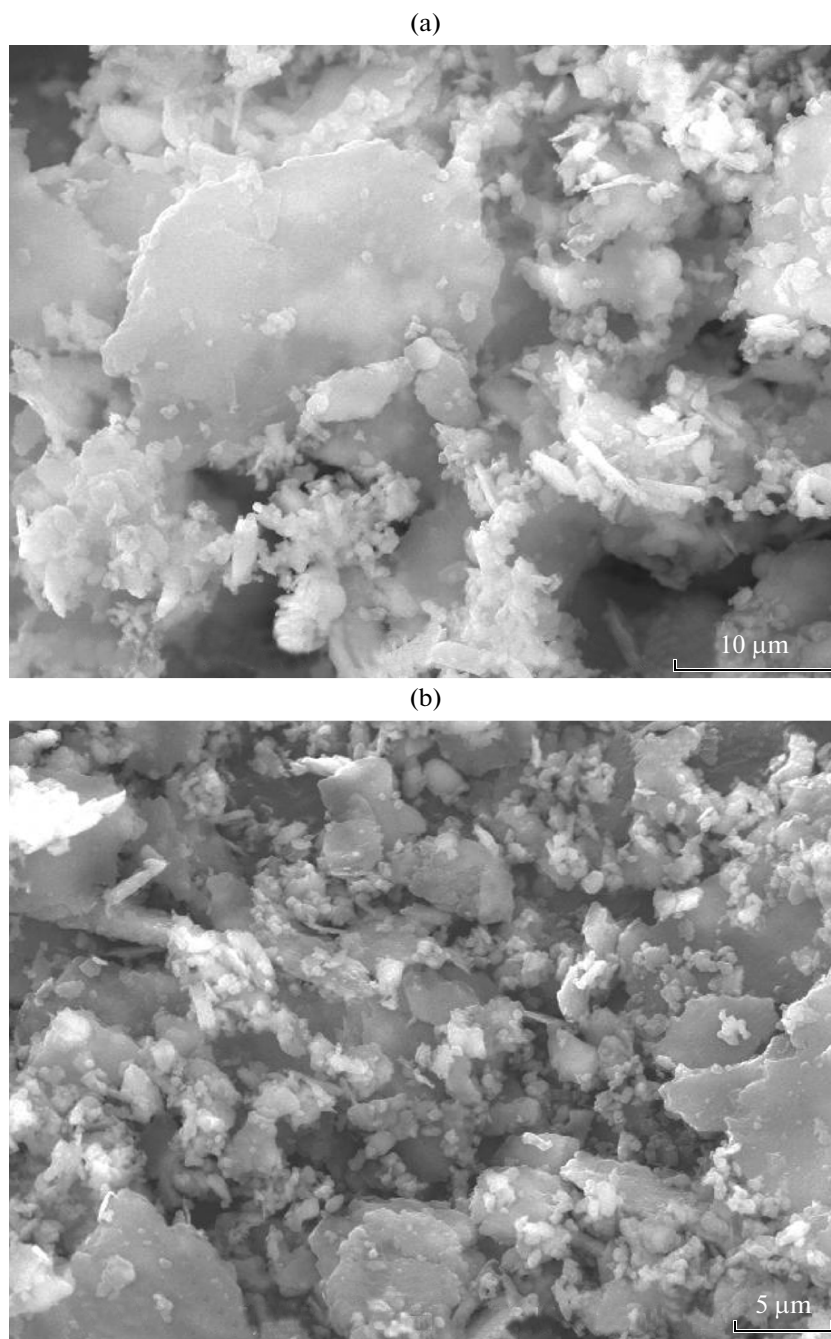


**Fig. 1.** Microphotographs of 40 : 60 Al/PP composites mechanoactivated for 30 min: (a) ASD-6-based and (b) PP-2-based.

X-ray diffraction analysis showed that, at activation times shorter than 30 min, no chemical reaction between the components occurs. The diffractograms featured the presence of only two phases: PP and Al. In addition, traces of Fe in a concentration of a few fractions of a percent were detected. The admixture of Fe in the product arises due to the attrition wear of the steel drums and balls.

Electron microscopy analysis showed that the mechanoactivated composites prepared from PP-2 Al

powder were generally more homogeneous as compared to the ASD-6-based ones. As an example, Fig. 1 displays SEM images of Al(ASD-6)/PP and Al(PP-2)/PP 40/60 composites with the same composition, but different grades of aluminum powder. In both cases, at a given activation time, PP particles are ground to a sub-micron size dimensions, but Al particles are crushed differently. While ASD-6 particles are deformed to form sufficiently large particles (“tablets” a few microns in size), located separately from PP grains, in

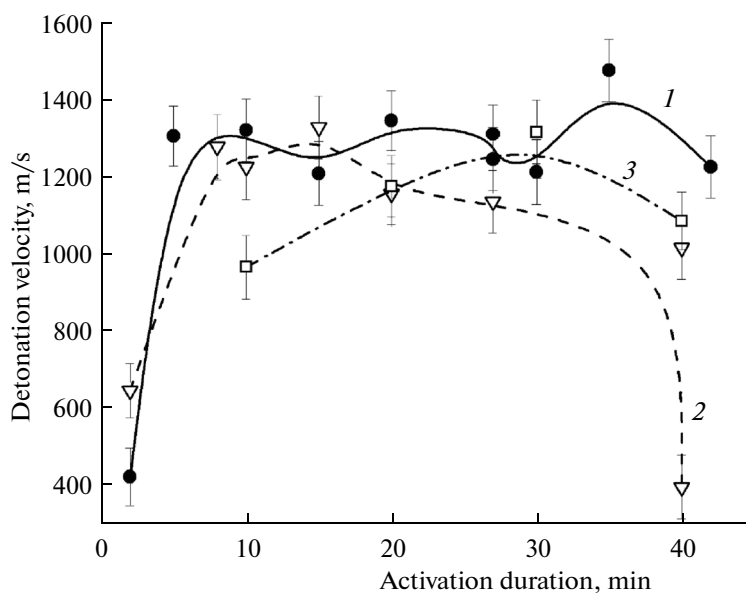


**Fig. 2.** Dependence of the detonation velocity on the activation duration for Al/PP composites of various compositions: (1) 30 : 70, (2) 35 : 65, and (3) 40 : 60 (in 80%-porosity charges placed in 10-mm-diameter steel tubes).

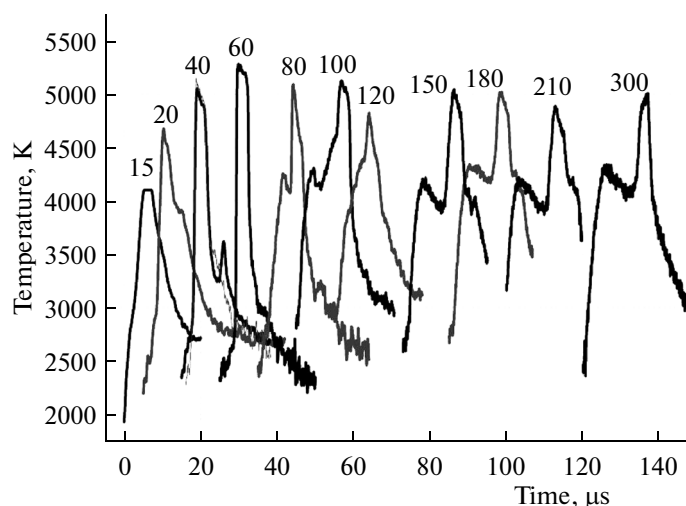


**Fig. 3.** Time profiles of the brightness temperature of the detonation products at the charge-PMMA window boundary for 30 : 70 Al/PP mechanoactivated composite charges of various lengths. The numbers at the profiles indicate the charge length in mm.

the case of PP-2 Al particles, more homogeneous composites arise, in the form of micron- and submicron-sized fragments of Al flakes coated with oxidant.

The MAEC under study were tested for deflagration-to-detonation transition and mechanical impact sensitivity. The experiments on deflagration-to-detonation transition were performed in steel tubes with a diameter of 10 mm and a length of 200 mm at a charge porosity of ~80%. The test mixture was poured into the tube in portions and tamped with a metal rod to ensure that the charges be of the same density. The burning was initiated with an electrically heated Nichrome wire located near the closed end of the tube.

The velocity of the combustion wave front was measured by recording the light emission of from the combustion products transmitted through optical fibers to photodiodes. The optical fibers were introduced through holes in the tube walls to the axis of the charge, a configuration that excluded the effect of a possible flashback along the walls of the tube. The velocity was measured over 20-mm measurement distances, starting from a point located at a distance of 70 mm from the initiation locus. Inspection of the tubes after the experiments made it possible to determine the deflagration-to-detonation transition length  $L$  and the steady detonation velocity  $D$ . Depending on

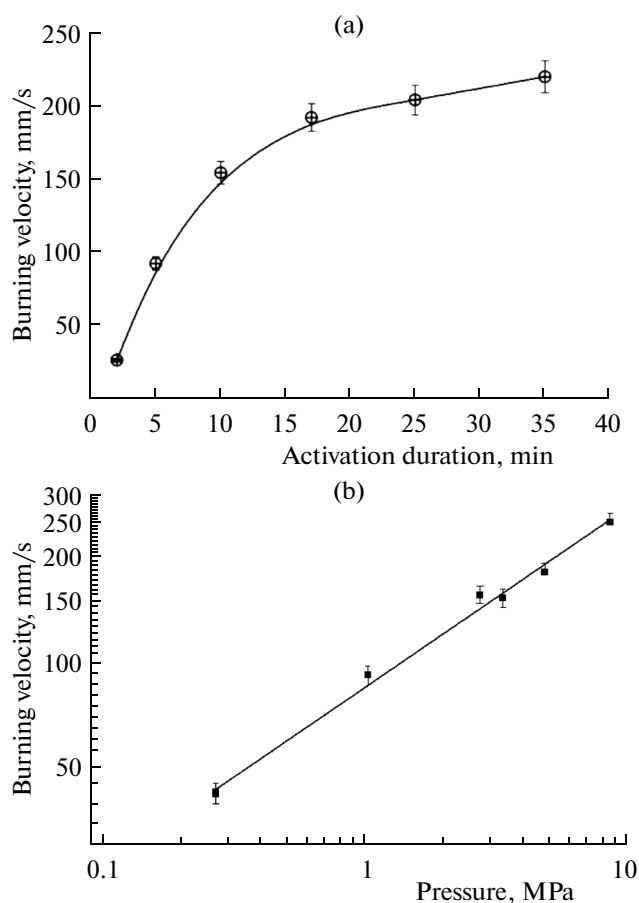


**Fig. 4.** Dependences the burning velocity of pressed samples of 30 : 70 Al/PP mechanoactivated composites on (a) the activation duration at the pressure of 3 MPa and (b) the pressure at the activation duration of 10 min;  $U$  [mm/s] =  $84.2(P$  [MPa])<sup>0.51</sup>.

the activation time and the composition of the composite, the value of  $L$  ranged from 10 to 80 mm, whereas  $D$  from 1200 to 1500 m/s. For PP-2-based MAEC, the detonation velocity was higher while the deflagration-to-detonation transition length shorter as compared to ASD-6-based MAEC, all other things being equal. This is consistent with a higher homogeneity of PP-2-based composites, as noted above.

Therefore, most of the subsequent experiments were performed with PP-2-based MAEC. Figure 2 show how the detonation velocity  $D$  depends on the composition of the composite and  $T_{act}$ . At  $T_{act} = 2$  min (charge length 200 mm), no deflagration-to-detonation transition was observed—only explosive combustion at 400–600 m/s took place, with the tube remaining practically undamaged. At  $T_{act} = 5$  min or more, deflagration-to-detonation transition occurred. The maximum value of  $D$  was obtained for composites with a slight excess of oxidizer, at Al : PP = 30 : 70. At  $T_{act}$  to 40 min or more,  $D$  decreased markedly, which may be a consequence of the components having reacted during mechanoactivation. Despite a rather large scatter in the data, the results suggest that the optimal treatment time ranges within  $T_{act} = 10$ –20 min. Most of the experiments were carried out with composites stored for 7–10 days. Increasing the storage time to 2–3 weeks did not affect the rates of the processes.

The formation of the detonation front in the course of propagation of the combustion wave along the charge was investigated by monitoring the visible emission from the products. The experiments were conducted with 80- to 82%-porosity charges in a duralumin tube of diameter 18 mm. The burning of the composite was initiated by an electrically heated Nichrome wire placed at one end of the tube. At the other end of the tube, an optical window was mounted (plates of polymethylmethacrylate (PMMA), 8-mm-thick LiF, 30-mm K-8 glass). The intensity of the radiation from the detonation products at the interface with the window was recorded with a two-channel pyrometer equipped with 627- and 420-nm-peak interference filters and then converted into the brightness temperature using standard procedures [5]. The measured dependence of the brightness temperature at the interface between an Al : PP = 30 : 70 composite (activation time  $T_{act} = 10$  min) and the PMMA windows on the length of the charge is shown in Fig. 3. The temperature values were obtained by averaging over the two wavelengths. The error in determination of the brightness temperature did not exceed the instrument error,  $\pm 150$  K. The numbers in the figure indicate the charge length; the temperature profiles

Results of the thermodynamic calculations of the ideal detonation parameters for a PP + 30% Al mixture at initial densities from 300 to 700 kg/m<sup>3</sup>

Initial density, kg/m <sup>3</sup>	Chapman–Jouguet detonation parameters			Detonation velocity, m/s
	density, kg/m <sup>3</sup>	pressure, GPa	speed of sound, m/s	
300	483	0.34	1080	1735
400	617	0.52	1220	1900
500	762	0.74	1360	2070
600	897	1.0	1500	2245
700	1028	1.31	1650	2420

are shifted along the time scale and arranged in accordance with the charge length.

As compared to MAEC prepared from nanosized silicon and ammonium perchlorate *n*Si/AP [3], a detonationlike process in Al/PP MAEC sets in much faster. In particular, at a length as short as ~20 mm, the signal intensity increases sharply (with a rise time of  $t < 5 \mu\text{s}$ ), with shock wave with a sufficiently steep front ( $t < 1.5 \mu\text{s}$ ) arising at a distance of 40 mm. At a length of 60 mm, the signal amplitude reaches a maximum, and  $t$  becomes less than  $1 \mu\text{s}$ . At longer distances, the signal reduces slightly whereas its rise time increases; at a distance of 150 mm, the characteristics of the process become roughly constant, with the temperature profile exhibiting a two-peak pattern.

With the LiF window, having a higher dynamic impedance compared to PMMA, the maximum temperature in the peak increases somewhat. With the thick K-8 glass window, no two-peak structure is observed. Why two-peak temperature profiles are observed remains unclear. It can be supposed that the first peak is associated with the burnout of the highly activated part of the mixture on the surface of aluminum particles; however, why the peak is not recorded in the case of the "thick" window is hard to say. In general, based on measuring the emission from the products at the end face of charges of different lengths, it can be assumed that the deflagration-to-detonation transition in high-porosity charges of mechanoactivated Al/PP composites occurs through the stage of overdriven detonation.

Since preliminary experiments on deflagration-to-detonation transition in 10-mm-diameter tubes showed no effect of overdriven detonation, to elucidate whether the stage of overdriven detonation exists, we carried out new experiments with 18-mm-diameter 300-mm-long tubes, in which the velocity of the wave was measured with a set of contact sensors placed at 20-mm intervals. The measurements have shown that, during the onset of detonation, the velocity of the wave reaches a maximum value of 2000 m/s within the 40–60-mm measurement distance, after which the wave velocity gradually reduces to 1500 m/s, remaining at this level constant up to the end of the charge. This result confirms the assumption that the onset of detonation in Al/PP charges occurs through the stage of overdriven detonation.

For Al : PP = 30 : 70 pressed charges, we also measured the layer-by-layer burning velocity. The charges, 12 mm in height and 9 mm diameter, were prepared by pressing to a relative density of 0.85–0.9. The lateral surface of the charges was coated with a thin layer of epoxy resin. The charges were burnt in a constant-volume bomb under nitrogen at pressures of 0.5 to 8.0 MPa. Burning was initiated with an incandescent coil. The burning time of the charge was determined from the time history of pressure in the bomb. The average burning velocity was calculated by dividing the charge height by the burning time. The data obtained,

in the form of the dependences of the burning velocity on the activation time (at an initial pressure in the bomb of 2 MPa) and on the initial pressure in the bomb (at  $T_{\text{act}} = 10 \text{ min}$ ), are displayed in Fig. 4. As can be seen, with  $T_{\text{act}}$  increasing from 2 to 17 min, the burning velocity increases sharply, from 25 to 200 mm/s; however, with a further increase in  $T_{\text{act}}$ , the burning velocity growth slows down. The highest value of the burning velocity, 220 mm/s, was obtained at  $T_{\text{act}} = 30 \text{ min}$ . The dependence of the burning velocity on the pressure at  $T_{\text{act}} = 10 \text{ min}$  can be represented as  $U [\text{mm/s}] = 84.2(P [\text{MPa}])^{0.51}$  (burning velocity, in mm/s; pressure, in MPa).

In general, the available data on the burning velocity of pressed composites show that mechanoactivation enables to vary this parameter over a wide range and to reach record velocities of combustion of pyrophoric compounds (burning velocity of unactivated formulations typically does not exceed 10 mm/s). A sufficiently strong pressure dependence of the burning velocity of activated composites indicates that a large amount of intermediate combustion products is produced in gaseous form, despite the fact that, at room temperature, the final combustion products ( $\text{Al}_2\text{O}_3$  and KCl) exist in the condensed state.

We also studied the sensitivity of mechanoactivated Al/PP composites to friction. The experiments were performed as described in [4], on a K-44-III pendulum impact testing machine. The test conditions conformed to the *GOST R50835-95* state standard: the sample weight was 20 mg, the roller displacement, 1.5 mm, the pendulum drop angle,  $90^\circ$ . The sensitivity was characterized by the lower limit of sensitivity to friction  $P_{\parallel}$ . This parameter was defined as the maximum contact pressure in a series of 10 experiments in which no one explosion occurred. The step of variation of the contact pressure was 5.0 MPa. The effects of aging and activation time on  $P_{\parallel}$  were examined. The results are shown in Figs. 5 and 6.

As can be seen from Fig. 5, freshly prepared composites (storage time, 4 days) are most sensitive. The value of  $P_{\parallel}$  for such a composite is very low, only 5 MPa, which is considerably less than the lower sensitivity limit of lead azide,  $P_{\parallel} = 30 \text{ MPa}$  [6]. The effect of aging (an increase in the lower sensitivity limit due to passivation during exposure to air) manifests itself within the first six weeks after the preparation of the composite. A further storage does not lead to a change in  $P_{\parallel}$ , which remains at a level of 24 MPa, indicative of an extremely high sensitivity to friction. The explosive conversion of the composites upon shear displacement was accompanied by a strong sound effect and a bright flash. During the tests, an explosive conversion in the detonation mode occurred one time, causing the destruction of the striker pin. For comparison, Fig. 5 shows a similar dependence of  $P_{\parallel}$  on the storage time for *n*Si/PP mixtures. It is seen that the aluminum composites are more sensitive to shear friction than the composites containing nanoscale silicon.

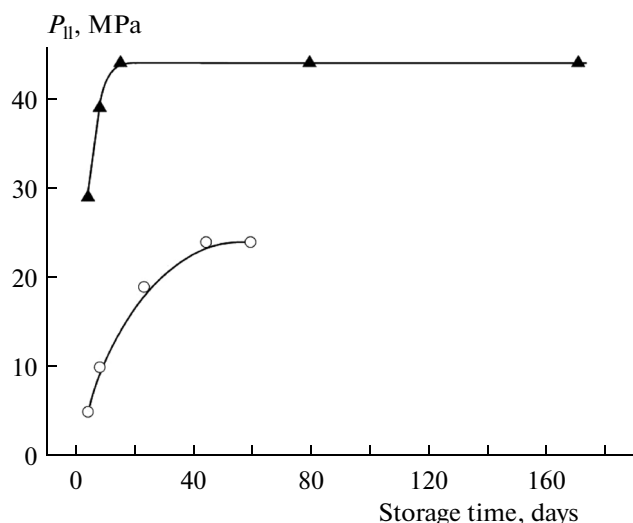


Fig. 5. Effect of aging on the lower limit  $P_{II}$ : (○) 30 : 70 Al/PP composite ( $T_{act} = 10$  min) and (▲) 30 : 70 nSi/PP composite [3].

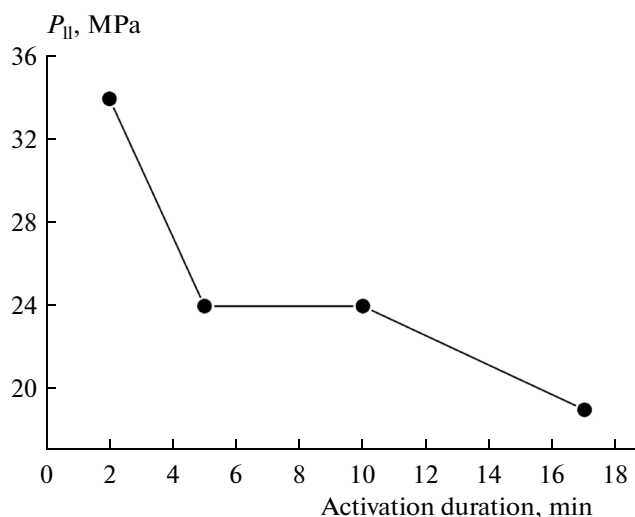


Fig. 6. Dependence of the lower limit  $P_{II}$  on the duration of activation of the 30 : 70 Al/PP composite.

The experimental dependence of  $P_{II}$  on the activation time is displayed in Fig. 6. In these experiments, formulations aged for 56–59 days after preparation were used. In general, with increasing activation time,  $P_{II}$  distinctly reduces. It is noteworthy that even a “soft” mechanoactivation treatment, for 2 min, produces composites with sensitivity similar to that of lead azide. Note that the increase of the treatment time from 5 to 10 min did not affect the lower limit sensitivity. However, a further elongation of the treatment time causes an increase in sensitivity; in particular, for an activation time of 17 min,  $P_{II} = 19$  MPa, which is higher than the sensitivity of lead azide.

## THEORY

Numerical simulations were performed using the quasi-one-dimensional-approximation program [7] developed for describing deflagration-to-detonation transition in porous energetic materials (EM). The model has been successfully applied to analyzing imperfect modes of the burning and detonation of black powder [8], the properties of which are formally close to those of the composition under study. The underlying concepts, governing equations, and the method of their numerical integration can be found in the cited papers—here, we will limit ourselves only to a brief description.

Consider a cylindrical EM charge consisting of spherical particles of the same diameter. As regards mechanoactivated composites, it is assumed that aluminum and PP particles, mixed at the nanoscale level, form aggregates of several tens of microns in size. The charge is placed into a steel shell with closed ends. At the initial moment, a small part of the charge adjacent to one end of the shell begins to burn at the surface of

the particles. This qualitatively reproduces the initiation of the charge with a wire coil inserted into the shell.

The combustion of particles yields hot products, which penetrate through pores (gaps between particles) into the unburnt part of the charge and ignite neighboring particles, thereby generating a combustion wave propagating along the charge. The propagation of the combustion wave was modeled within the framework of two-phase reaction medium mechanics. The EM particles comprise the solid phase. The combustion products, along with the gas initially filling the pores, constitute the gas phase. The volume fraction of the gas phase, or porosity  $\phi$ , determines the ratio between the medium phases. Each phase has its own internal energy, temperature, density, and flow rate, being described by its own equation of state (two-term equations with constant Grüneisen for the gas phase and the Tait equation for the compressibility of the solid phase [9]). The pressure in the solid phase differs from the gas pressure by an amount determined by the intergranular interaction between EM particles reacting with each other. All the characteristics of the phases, as is customary in continuum mechanics, are obtained by formally averaging over a volume containing a large number of EM particles.

An EM particle in the combustion wave ignites when its surface temperature reaches the preset ignition temperature. The particles are heated by convective heat transfer from the hot gas and due to the viscoplastic collapse of pores. These factors may act together or separately. Combustion occurs at the outer surface of the particles, with the mass burning rate being equal to the product of the layer-by-layer burning velocity (a function of pressure) and the specific surface of the particles.

The simulations were performed at two levels. The macroscopic level is represented by the equations of mass, momentum, energy, and state for a two-phase medium. The mesoscopic level is represented by a unit cell that imitates a pore and the adjacent EM layer. The heat conduction equation for the cell describes the temperature distribution and heat generation in the viscoplastic layer around the pore; it is used to determine the ignition time.

The model takes into account the following processes: the filtration flow of gas in the pores; convective heat transfer from the gas to the particulate material surface; movement of the solid phase under the influence of stresses, leading to compaction (porosity reduction) and viscoplastic heating of the solid phase; ignition and combustion of the particles; and radial plastic expansion of the shell channel (in a quasi-one-dimensional approximation) when the pressure becomes higher than the tensile strength of the shell.

The problem is solved numerically using the tridiagonal finite-difference scheme in conjunction with splitting into the macroscopic and mesoscopic levels. The computational grid along the charge, homogeneous at the initial time, is transformed during computation, being refined in areas where the gradients of the variables increase and coarsened where the gradients decrease. At the mesoscopic level, the computational grid over the thickness of the cell web originates at the inner boundary of the cell and has a step increasing in geometric progression with distance from this boundary.

The calculation was performed for a Al : PP = 30 : 70 mechanoactivated composite. Let us consider the main input parameter of the calculation. The equation of state of the detonation products of the mixture reads as

$$P = \Gamma \rho_g (e_g - e_0) + B \rho_g^m \left( 1 - \frac{\Gamma}{m-1} \right). \quad (1)$$

Here,  $P$  is the pressure, and  $\rho_g$  and  $e_g$  are the density and internal energy of the detonation products. The equation includes four constants: the Grüneisen coefficient  $\Gamma$ , chemical energy  $e_0$ , and the coefficients  $m$  and  $B$ , which characterize the potential component of the pressure of the detonation products. To determine these constants, we used the results of thermodynamic calculations of the detonation parameters for this composition. The calculations were carried out using the DNITERM program [10] with the BKWR equation of state. The calculation results at initial densities from 300 to 700 kg/m<sup>3</sup>, which covers the expected range of characteristics, are listed in the table. The value of  $e_0$ , average for the density interval is 6.3 MJ/kg; the detonation temperature is slightly above 5500 K. The equilibrium composition of the detonation products (in mol/kg) was found to consist of aluminum oxide Al<sub>2</sub>O<sub>3</sub> (5.55) and gaseous components, such as O<sub>2</sub> (1.86), KCl (3.4), K<sub>2</sub>Cl<sub>2</sub> (0.51), KO (0.73), K (0.12) and Cl (0.71). The fractions of the remaining gas components, including aluminum-containing ones, did not exceed 0.01 mol/kg.

The coefficients of Eq. (1) were selected in such a way as to achieve the best agreement with the characteristics listed in the table at a given value of  $e_0$ . The values of coefficients used in the numerical simulation are  $\Gamma = 0.07$ ,  $m = 2.718$ , and  $B = 4.578$ .

The compressibility of the condensed phase in this pressure range (up to 1 GPa) can be presented in the linear form:

$$\rho_k / \rho_{k0} = 1 + P_S / K. \quad (2)$$

Here,  $K$  is the compression modulus of the mixture, which is additively calculated from compression modules and volume fractions of the components (for the studied mixture with 30 wt % Al,  $K = 25$  GPa);  $P_S$  is the sum of the gas pressure  $P$  and intergranular stress  $P_c$  (arising due to the interaction of c-phase particles with each other). The intergranular stress is a function of the porosity  $\phi$ , which is defined as follows. For the porosity range from 1 to the value corresponding to the pour density (for the given composite,  $\phi = 0.8$ ),  $P_c = 0$ . In the range from the pour-density porosity to  $\phi = 0.05$ , the intergranular stress is determined from a static experiment on a press. For the composite under study  $P_c$  [MPa] = 120(1 -  $\phi/0.8$ )<sup>3</sup>. At a lower porosity, the function  $P_c$  [MPa] = 5/ $\phi$  is used, which provides the unlimited increase of the stress as the porosity tends to zero.

The ignition temperature of the test mixture is not known exactly. The combustion of aluminum needs oxygen, which is released during the decomposition of PP. The primary event of abstraction of an oxygen atom is endothermic by about 287 kJ/mol. According to TGA analysis on a Netzsch STA 449 Jupiter thermal analyzer equipped with a Aeolos mass spectrometer at heating rate of 10 K/min, the decomposition of original PP starts at ~840 K, whereas for mechanoactivated PP, this temperature is ~740 K. In our calculations, the ignition temperature was 1000 K, whereas the average heat capacity of the composite, 1.5 kJ/(kg K).

After ignition, burning occurs at the outer surface of composite particles at the layer-by-layer burning velocity, which was measured to be described by the expression  $U_p$  [mm/s] = 84.2( $P$  [MPa])<sup>0.51</sup> at an activation time of 10 min. This dependence was extrapolated to the entire range of pressures, up to 1 GPa. Material particles were aggregates of mixture nanoparticles. In the calculations, the particle size was set equal to 20  $\mu$ m.

The shell of the charge was considered to be non-deformable until the pressure exceeds its tensile strength, which is calculated by the formula  $P_W = Y \ln(1 + H_c/R_c)$ . Here,  $H_c$  and  $R_c$  are the shell thickness and initial channel radius, which were assumed to be 1 and 5 mm, respectively;  $Y$  is the yield strength of the shell material, the value of which, with allowance for dynamic strengthening, was taken to be 700 MPa. At higher pressures, the shell was assumed to expand in the real plasticity mode.

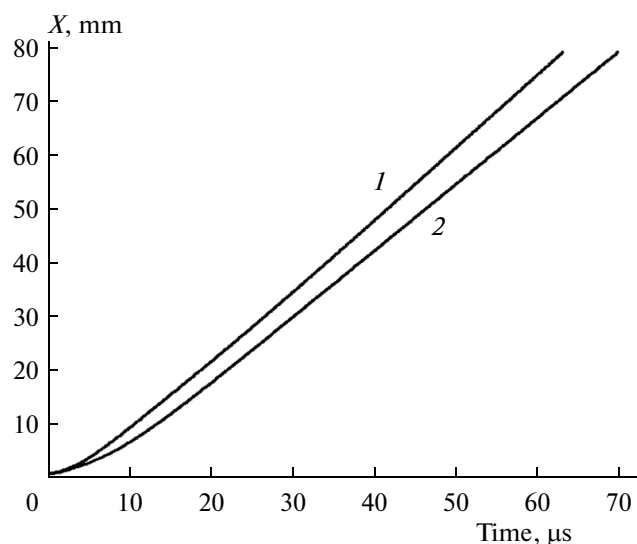


Fig. 7. Calculated trajectories of the wave for composites with grain diameters of (1) 20 and (2) 40  $\mu\text{m}$ .

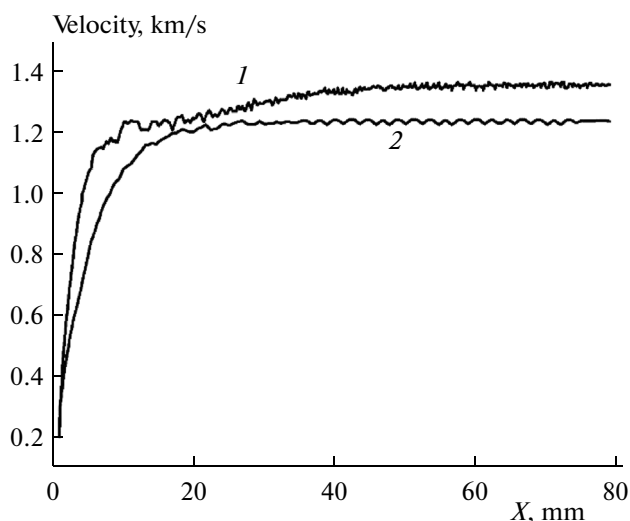


Fig. 8. Calculated dependences of the wave velocity on the distance traversed for composites with grain diameters of (1) 20 and (2) 40  $\mu\text{m}$ .

The calculation results are shown in Figs. 7–10. For calculations at a grain diameter of 20  $\mu\text{m}$ , which was chosen as a reference, the trajectory wavefront (Fig. 7), the wave velocity (Fig. 8), and the maximum values of the pressure and mass flow rate for the gaseous and condensed phases behind the wave as functions of the distance traversed (Fig. 9) are shown. Before reaching the steady mode of propagation, the wave passes through two stages of evolution. Immediately after initiation, the wave accelerates quickly, with

the characteristics of the wave reaching 80% of their steady-state values already at a distance of 10 mm. The subsequent, much slower growth ends at a distance of  $\sim 50$  mm. There is agreement with experiment in the predetonation length (no more than 10 mm) and detonation velocity ( $\sim 1.36$  km/s). Note, however, that the calculations do not predict the stage of overdriven detonation observed in the experiment.

Typical spatial profiles of the main characteristics of the wave when it reached the steady state are shown

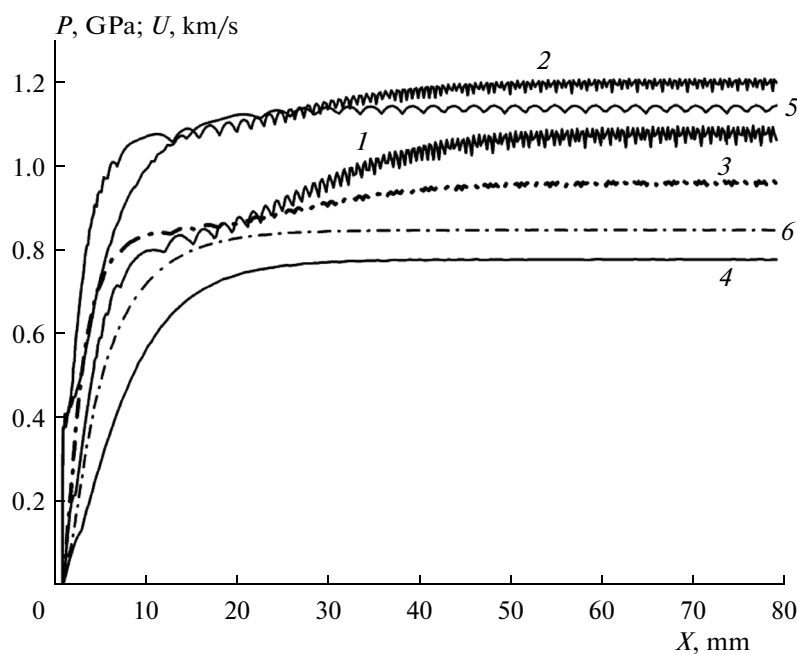


Fig. 9. Calculated dependences of the maximum values of the (1, 4) pressure, (2, 5) gas velocity, and (3, 6) c-phase velocity on the distance traversed for composites with grain diameters of (1–3) 20 and (4–6) 40  $\mu\text{m}$ .



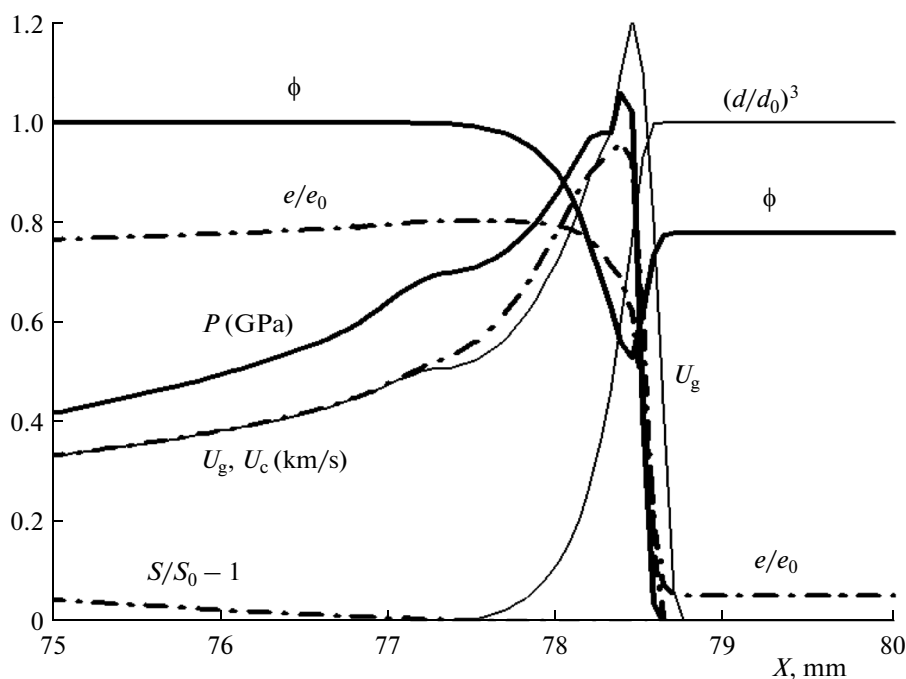


Fig. 10. Calculated spatial profiles of the wave at time 62.5  $\mu\text{s}$  for a composite with a grain diameter of 20  $\mu\text{m}$ .

in Fig. 10. Here,  $P$  is the pressure,  $\phi$  is the porosity,  $U_g$  is the velocity of the gas phase,  $U_c$  is the velocity of the condensed phase,  $e/e_0$  is the internal energy of the gas referred to the chemical energy of the composite,  $(d/d_0)^3$  is the fraction of unburnt composite, and  $(S/S_0 - 1)$  is the relative expansion of the cross section of the shell channel. The results displayed in Fig. 10 demonstrate a leading growth of the gas velocity compared to the gas pressure rise and c-phase velocity growth (by  $\sim 0.15\text{mm}$ ). The ignition of the composite occurs in the wave front before the maximum pressure is reached. The reaction zone width is  $\sim 1\text{ mm}$ . The calculated peak values of the pressure, gas velocity, and c-phase are 1.1 GPa, 1.2 km/s, and 0.95 km/s.

The graphs also display the calculation results for a version in which the grain size was doubled, to 40  $\mu\text{m}$ . The characteristics of the wave in the steady mode are lower: detonation velocity, 1.23 km/s; peak pressure, 0.78 GPa; and predetonation length, 20 mm.

Thus, the numerical simulation results on the dynamics of evolution of the blast wave and the steady detonation velocity are in qualitative agreement with the experimental data. However, thermodynamic calculations suggest that the detonation velocity is significantly (by almost 40%) lower rate than the normal detonation velocity. Such a strong deviation the non-ideal detonation velocity from the thermodynamically calculated value can be accounted for by various reasons, including a relatively weak pressure dependence of the burning rate. However, to achieve full understanding of these aspects, additional studies, including those with charges of larger diameters, are needed.

## CONCLUSIONS

The properties of mechanoactivated aluminum–potassium perchlorate energetic composites were studied. The experimental results on the burning, deflagration-to-detonation transition, and sensitivity to friction of these composites were examined. The activation duration and aluminum content in the mixture were varied. The results obtained suggest mechanoactivation is an effective method for controlling the burning rate and deflagration-to-explosion transition, while mechanoactivated aluminum–potassium perchlorate composites may be of interest as promising energetic materials for new ignition and incendiary formulations with high demands on the energy release rate.

Experiments on deflagration-to-detonation transition in mechanoactivated composites were supplemented by the results of numerical simulation and thermodynamic calculations. The observed velocity of the detonation process was found to considerably (by nearly 40%) lower than the normal detonation velocity obtained from thermodynamic calculations. The numerical simulation results are in qualitative agreement with the experimental data on the dynamics of the blast wave and the steady detonation velocity.

## ACKNOWLEDGMENTS

The authors are grateful to N.E. Safronov for help with the experiments.

The work was supported by the Russian Foundation for Basic Research, project no. 12-03-00651.

#### REFERENCES

1. A. Yu. Dolgoborodov, M. N. Makhov, A. N. Streletskii, et al., in *Proceedings of the EUROPYRO 2011 Conference* (Reims, France, 2011), p. 1/9.
2. A. Yu. Dolgoborodov, M. N. Makhov, A. N. Streletskii, et al., in *Combustion and Explosion*, Ed. by S. M. Frolov (Torus Press, Moscow, 2011), No. 4, p. 330 [in Russian].
3. A. Yu. Dolgoborodov, A. N. Streletskii, M. N. Makhov, V. A. Teselkin, Sh. L. Guseinov, P. A. Storozhenko, and V. E. Fortov, *Russ. J. Phys. Chem. B* **6**, 523 (2012).
4. V. A. Teselkin, A. N. Streletskii, I. V. Kolbanev, and A. Yu. Dolgoborodov, in *Combustion and Explosion*, Ed. by S. M. Frolov (Torus Press, Moscow, 2010), No. 3, p. 292 [in Russian].
5. D. Ya. Svet, *Optical Methods of True Temperature Measurement* (Nauka, Moscow, 1982) [in Russian].
6. *Recommendations on the Transport of Dangerous Goods. Manual of Tests and Criteria*, 5th rev. ed., ST/SG/AC 10/11/Rev.5 (United Nations, New York, Geneva, 2009).
7. B. S. Ermolaev, A. A. Belyaev, and A. A. Sulimov, *Khim. Fiz.* **23** (1), 62 (2004).
8. B. S. Ermolaev, A. A. Belyaev, S. B. Viktorov, K. A. Sleptsov, and S. Yu. Zharikova, *Russ. J. Phys. Chem. B* **4**, 428 (2010).
9. *Explosion Physics*, Ed. by L. P. Orlenko (Fizmatlit, Moscow, 2002) [in Russian].
10. N. A. Imkhovik and V. S. Solov'ev, *Vestn. Mosk. Tekh. Univ., Ser. Mashinostr.*, No. 2, 53 (1993).

*Translated by V. Smirnov*